

1 **A GENERALISED RANDOM ENCOUNTER MODEL FOR ESTIMATING**
2 **ANIMAL DENSITY WITH REMOTE SENSOR DATA**

3 **Running title: A generalised random encounter model for animals.**

4 **Word count:** 7154

5 **Authors:**

6 Tim C.D. Lucas^{1,2,3,†}, Elizabeth A. Moorcroft^{1,4,5,†}, Robin Freeman⁵, Marcus J. Rowcliffe⁵,
7 Kate E. Jones^{2,5}

8 **Addresses:**

9 1 CoMPLEX, University College London, Physics Building, Gower Street, Lon-
10 don, WC1E 6BT, UK

11 2 Centre for Biodiversity and Environment Research, Department of Genetics,
12 Evolution and Environment, University College London, Gower Street, London,
13 WC1E 6BT, UK

14 3 Department of Statistical Science, University College London, Gower Street,
15 London, WC1E 6BT, UK

16 4 Department of Computer Science, University College London, Gower Street,
17 London, WC1E 6BT, UK

18 5 Institute of Zoology, Zoological Society of London, Regents Park, London, NW1
19 4RY, UK

20 † First authorship shared.

21 **Corresponding authors:**

22 Kate E. Jones,
23 Centre for Biodiversity and Environment Research,
24 Department of Genetics, Evolution and Environment,
25 University College London,
26 Gower Street,
27 London,
28 WC1E 6BT,

29 UK

30 kate.e.jones@ucl.ac.uk

31

32 Marcus J. Rowcliffe,

33 Institute of Zoology,

34 Zoological Society of London,

35 Regents Park,

36 London,

37 NW1 4RY,

38 UK

39 marcus.rowcliffe@ioz.ac.uk

ABSTRACT

1: Wildlife monitoring technology is advancing rapidly and the use of remote sensors such as camera traps and acoustic detectors is becoming common in both the terrestrial and marine environments. Current methods to estimate abundance or density require individual recognition of animals or knowing the distance of the animal from the sensor, which is often difficult. A method without these requirements, the random encounter model (REM), has been successfully applied to estimate animal densities from count data generated from camera traps. However, count data from acoustic detectors do not fit the assumptions of the REM due to the directionality of animal signals.

2: We developed a generalised REM (gREM), to estimate absolute animal density from count data from both camera traps and acoustic detectors. We derived the gREM for different combinations of sensor detection widths and animal signal widths (a measure of directionality). We tested the accuracy and precision of this model using simulations of different combinations of sensor detection widths and animal signal widths, number of captures, and models of animal movement.

3: We find that the gREM produces accurate estimates of absolute animal density for all combinations of sensor detection widths and animal signal widths. However, larger sensor detection and animal signal widths were found to be more precise. While the model is accurate for all capture efforts tested, the precision of the estimate increases with the number of captures. We found no effect of different animal movement models on the accuracy and precision of the gREM.

4: We conclude that the gREM provides an effective method to estimate absolute animal densities from remote sensor count data over a range of sensor and animal signal widths. The gREM is applicable for count data obtained in both marine and terrestrial environments, visually or acoustically (e.g., big cats, sharks, birds, echolocating bats and cetaceans). As sensors such as camera traps and acoustic detectors become more ubiquitous, the gREM will be increasingly useful for monitoring unmarked animal populations across broad spatial, temporal and taxonomic scales.

Keywords. Acoustic detection, camera traps, marine, population monitoring, simulations, terrestrial

INTRODUCTION

Animal population density is one of the fundamental measures in ecology and conservation. The density of a population has important implications for a range of issues such as sensitivity to stochastic fluctuations (Richter-Dyn & Goel, 1972; Wright & Hubbell, 1983) and risk of extinction (Purvis *et al.*, 2000). Monitoring animal population changes in response to anthropogenic pressure is becoming increasingly important as humans rapidly modify habitats and change climates (Everatt *et al.*, 2014). Sensor technology, such as camera traps (Karanth, 1995; Rowcliffe & Carbone, 2008) and acoustic detectors (Clark, 1995; Acevedo & Villanueva-Rivera, 2006; Walters *et al.*, 2012) are becoming widely used to monitor changes in animal populations (Rowcliffe & Carbone, 2008; Kessel *et al.*, 2014; Walters *et al.*, 2013), as they are efficient, relatively cheap and non-invasive (Cutler & Swann, 1999), allowing for surveys over large areas and long periods. However, converting sampled count data into estimates of density is problematic as detectability of animals needs to be accounted for (Anderson, 2001).

Existing methods for estimating animal density often require additional information that is often unavailable. For example, capture-mark-recapture methods (Karanth, 1995; Trolle *et al.*, 2007; Borchers *et al.*, 2014) require recognition of individuals, and distance methods (Harris *et al.*, 2013) require an estimation of how far away individuals are from the sensor (Barlow & Taylor, 2005; Marques *et al.*, 2011). More recently, the development of the random encounter model (REM) (a modification of a gas model) has enabled animal densities to be estimated from unmarked individuals of a known speed, and with known sensor detection parameters (Rowcliffe *et al.*, 2008). The REM method has been successfully applied to estimate animal densities from camera trap surveys (Manzo *et al.*, 2012; Zero *et al.*, 2013). However, extending the REM method to other types of sensors (e.g., acoustic detectors) is more problematic, because the original derivation assumes a relatively narrow sensor width (up to $\pi/2$ radians) and that the animal is equally detectable irrespective of its heading (Rowcliffe *et al.*, 2008).

101 Whilst these restrictions are not problematic for most camera trap makes (e.g.,
102 Reconyx, Cuddeback), the REM cannot be used to estimate densities from camera
103 traps with a wider sensor width (e.g. canopy monitoring with fish eye lenses,
104 Brusa & Bunker (2014)). Additionally, the REM method is not useful in estimating
105 densities from acoustic survey data as acoustic detector angles are often wider
106 than $\pi/2$ radians. Acoustic detectors are designed for a range of diverse tasks
107 and environments (Kessel *et al.*, 2014), which naturally leads to a wide range of
108 sensor detection widths and detection distances. In addition to this, calls emitted
109 by many animals are directional (Blumstein *et al.*, 2011), breaking the assumption
110 of the REM method.

111 There has been a sharp rise in interest around passive acoustic detectors in re-
112 cent years, with a 10 fold increase in publications in the decade between 2000 and
113 2010 (Kessel *et al.*, 2014). Acoustic monitoring is being developed to study many
114 aspects of ecology, including the interactions of animals and their environments
115 (Blumstein *et al.*, 2011; Rogers *et al.*, 2013), the presence and relative abundances of
116 species (Marcoux *et al.*, 2011), biodiversity of an area (Depraetere *et al.*, 2012), and
117 monitoring population trends (Walters *et al.*, 2013).

118 Acoustic data suffers from many of the problems associated with data from
119 camera trap surveys in that individuals are often unmarked, so capture-mark-
120 recapture methods cannot be used to estimate densities. In some cases the dis-
121 tance between the animal and the sensor is known, for example when an array of
122 sensors is deployed and the position of the animal is estimated by triangulation
123 (Lewis *et al.*, 2007). In these situations distance-sampling methods can be applied,
124 a method typically used for marine mammals (Rogers *et al.*, 2013). However, in
125 many cases distance estimation is not possible, for example when single sensors
126 are deployed, a situation typical in the majority of terrestrial acoustic surveys (El-
127 phick, 2008; Buckland *et al.*, 2008). In these cases, only relative measures of local
128 abundance can be calculated, and not absolute densities. This means that compar-
129 ison of populations between species and sites is problematic without assuming
130 equal detectability (Hayes, 2000; Schmidt, 2003; Walters *et al.*, 2013). Equal de-
131 tectability is unlikely because of differences in environmental conditions, sensor
132 type, habitat, and species biology.

133 In this study, we create a generalised REM (gREM) as an extension to the cam-
 134 era trap model of Rowcliffe *et al.* (2008), to estimate absolute density from count
 135 data from acoustic detectors, or camera traps, where the sensor width can vary
 136 from 0 to 2π radians, and the signal given from the animal can be directional. We
 137 assessed the accuracy and precision of the gREM within a simulated environment,
 138 by varying the sensor detection widths, animal signal widths, number of captures
 139 and models of animal movement. We use the simulation results to recommend
 140 best survey practice for estimating animal densities from remote sensors.

141 METHODS

142 **Analytical Model.** The REM presented by Rowcliffe *et al.* (2008) adapts the gas
 143 model to count data collected from camera trap surveys. The REM is derived
 144 assuming a stationary sensor with a detection width less than $\pi/2$ radians. How-
 145 ever, in order to apply this approach more generally, and in particular to stationary
 146 acoustic detectors, we need both to relax the constraint on sensor detection width,
 147 and allow for animals with directional signals. Consequently, we derive the gREM
 148 for any detection width, θ , between 0 and 2π with a detection distance r giving a
 149 circular sector within which animals can be captured (the detection zone) (Fig-
 150 ure 1). Additionally, we model the animal as having an associated signal width
 151 α between 0 and 2π (Figure 1, see Appendix S1 for a list of symbols). We start
 152 deriving the gREM with the simplest situation, the gas model where $\theta = 2\pi$ and
 153 $\alpha = 2\pi$.

154 *Gas Model.* Following Yapp (1956), we derive the gas model where sensors can
 155 capture animals in any direction and animal signals are detectable from any direc-
 156 tion ($\theta = 2\pi$ and $\alpha = 2\pi$). We assume that animals are in a homogeneous environ-
 157 ment, and move in straight lines of random direction with velocity v . We allow
 158 that our stationary sensor can capture animals at a detection distance r and that if
 159 an animal moves within this detection zone they are captured with a probability
 160 of one, while animals outside the zone are never captured.

161 In order to derive animal density, we need to consider relative velocity from
 162 the reference frame of the animals. Conceptually, this requires us to imagine that
 163 all animals are stationary and randomly distributed in space, while the sensor

164 moves with velocity v . If we calculate the area covered by the sensor during the
 165 survey period, we can estimate the number of animals the sensor should capture.
 166 As a circle moving across a plane, the area covered by the sensor per unit time is
 167 $2rv$. The number of expected captures, z , for a survey period of t , with an animal
 168 density of D is $z = 2rvtD$. To estimate the density, we rearrange to get $D = z/2rvt$.

169 *gREM derivations for different detection and signal widths.* Different combinations of
 170 θ and α would be expected to occur (e.g., sensors have different detection widths
 171 and animals have different signal widths). For different combinations θ and α , the
 172 area covered per unit time is no longer given by $2rv$. Instead of the size of the
 173 sensor detection zone having a diameter of $2r$, the size changes with the approach
 174 angle between the sensor and the animal. For any given signal width and detec-
 175 tor width and depending on the angle that the animal approaches the sensor, the
 176 width of the area within which an animal can be detected is called the profile, p .
 177 The size of the profile (averaged across all approach angles) is defined as the aver-
 178 age profile \bar{p} . However, different combinations of θ and α need different equations
 179 to calculate \bar{p} .

180 We have identified the parameter space for the combinations of θ and α for
 181 which the derivation of the equations are the same (defined as sub-models in the
 182 gREM) (Figure 2). For example, the gas model becomes the simplest gREM sub-
 183 model (upper right in Figure 2) and the REM from Rowcliffe *et al.* (2008) is another
 184 gREM sub-model where $\theta < \pi/2$ and $\alpha = 2\pi$. We derive one gREM sub-model SE2
 185 as an example below, where $2\pi - \alpha/2 < \theta < 2\pi$, $0 < \alpha < \pi$ (see Appendix S2 for
 186 derivations of all gREM sub-models).

187 *Example derivation of SE2.* In order to calculate \bar{p} , we have to integrate over the
 188 focal angle, x_1 (Figure 3a). This is the angle taken from the centre line of the sensor.
 189 Other focal angles are possible (x_2, x_3, x_4) and are used in other gREM sub-models
 190 (see Appendix S2). As the size of the profile depends on the approach angle, we
 191 present the derivation across all approach angles. When the sensor is directly
 192 approaching the animal $x_1 = \pi/2$.

193 Starting from $x_1 = \pi/2$ until $\theta/2 + \pi/2 - \alpha/2$, the size of the profile is $2r \sin \alpha/2$
 194 (Figure 3b). During this first interval, the size of α limits the width of the profile.

When the animal reaches $x_1 = \theta/2 + \pi/2 - \alpha/2$ (Figure 3c), the size of the profile is $r \sin(\alpha/2) + r \cos(x_1 - \theta/2)$ and the size of θ and α both limit the width of the profile (Figure 3c). Finally, at $x_1 = 5\pi/2 - \theta/2 - \alpha/2$ until $x_1 = 3\pi/2$, the width of the profile is again $2r \sin \alpha/2$ (Figure 3d) and the size of α again limits the width of the profile.

The profile width p for π radians of rotation (from directly towards the sensor to directly behind the sensor) is completely characterised by the three intervals (Figure 3b–d). Average profile width \bar{p} is calculated by integrating these profiles over their appropriate intervals of x_1 and dividing by π which gives

$$\bar{p} = \frac{1}{\pi} \left(\int_{\frac{\pi}{2}}^{\frac{\pi}{2} + \frac{\theta}{2} - \frac{\alpha}{2}} 2r \sin \frac{\alpha}{2} dx_1 + \int_{\frac{\pi}{2} + \frac{\theta}{2} - \frac{\alpha}{2}}^{\frac{5\pi}{2} - \frac{\theta}{2} - \frac{\alpha}{2}} r \sin \frac{\alpha}{2} + r \cos \left(x_1 - \frac{\theta}{2} \right) dx_1 + \int_{\frac{5\pi}{2} - \frac{\theta}{2} - \frac{\alpha}{2}}^{\frac{3\pi}{2}} 2r \sin \frac{\alpha}{2} dx_1 \right) \quad \text{eqn 1}$$

$$= \frac{r}{\pi} \left(\theta \sin \frac{\alpha}{2} - \cos \frac{\alpha}{2} + \cos \left(\frac{\alpha}{2} + \theta \right) \right) \quad \text{eqn 2}$$

We then use this expression to calculate density

$$D = z/vt\bar{p}. \quad \text{eqn 3}$$

Rather than having one equation that describes \bar{p} globally, the gREM must be split into submodels due to discontinuous changes in p as α and β change. These discontinuities can occur for a number of reasons such as a profile switching between being limited by α and θ , the difference between very small profiles and profiles of size zero, and the fact that the width of a sector stops increasing once the central angle reaches π radians (i.e., a semi-circle is just as wide as a full circle.)

As an example, if α is small, there is an interval between Figure 3c and 3d where the ‘blind spot’ would prevent animals being detected giving $p = 0$. This would require an extra integral in our equation, as simply putting our small value of α into eqn 1 would not give us this integral of $p = 0$.

gREM submodel specifications were done by hand, and the integration was done using SymPy (SymPy Development Team, 2014) in Python (Appendix S3). The gREM submodels were checked by confirming that: (1) submodels adjacent in parameter space were equal at the boundary between them; (2) submodels that

border $\alpha = 0$ had $p = 0$ when $\alpha = 0$; (3) average profile widths \bar{p} were between 0 and $2r$ and; (4) each integral, divided by the range of angles that it was integrated over, was between 0 and $2r$. The scripts for these tests are included in Appendix S3 and the R (Team, 2014) implementation of the gREM is given in Appendix S4.

Simulation Model. We tested the accuracy and precision of the gREM by developing a spatially explicit simulation of the interaction of sensors and animals using different combinations of sensor detection widths, animal signal widths, number of captures, and models of animal movement. 100 simulations were run where each consisted of a 7.5 km by 7.5 km square with periodic boundaries. A stationary sensor of radius r was set up in the exact centre of each simulation, covering seven sensor detection widths θ , between 0 and 2π ($2/9\pi$, $4/9\pi$, $6/9\pi$, $8/9\pi$, $10/9\pi$, $14/9\pi$, and 2π). Each sensor was set to record continuously and to capture animal signals instantaneously from emission. Each simulation was populated with a density of 70 animals km^{-2} , calculated from the equation in Damuth (1981) as the expected density of mammals weighing 1 g. This density therefore represents a reasonable estimate of density of individuals, given that the smallest mammal is around 2 g (Jones *et al.*, 2009). A total of 3937 individuals per simulation were created which were placed randomly at the start of the simulation. Individuals were assigned 11 signal widths α between 0 and π ($1/11\pi$, $2/11\pi$, $3/11\pi$, $4/11\pi$, $5/11\pi$, $6/11\pi$, $7/11\pi$, $8/11\pi$, $9/11\pi$, $10/11\pi$, π).

Each simulation lasted for N steps (14400) of duration T (15 minutes) giving a total duration of 150 days. The individuals moved within each step with a distance d , with an average speed, v . d , was sampled from a normal distribution with mean distance, $\mu_d = vT$, and standard deviation $\sigma_d = vT/10$. An average speed, $v = 40 \text{ km day}^{-1}$, was chosen as this is the largest day range of terrestrial animals (Carbone *et al.*, 2005), and represents the upper limit of realistic speeds. At the end step, individuals were allowed to either remain stationary for a time step (with a given probability, S), or change direction (in a uniform distribution with a maximum angle, A) between 0 and π . This resulted in seven different movement models where: (1) simple movement, where S and $A = 0$; (2) stop-start movement, where (i) $S = 0.25$, $A = 0$, (ii) $S = 0.5$, $A = 0$, (iii) $S = 0.75$, $A = 0$; (3) random walk

250 movement, where (i) $S = 0, A = \pi/3$, (ii) $S = 0, A = 2\pi/3$, (iii) $S = 0, A = \pi$. Individuals
 251 were counted as they moved in and out of the detection zone of the sensor per
 252 simulation.

253 We calculated the estimated animal density from the gREM by assuming the
 254 number of captures per simulation and inputting these values into the correct
 255 gREM submodel. gREM accuracy was determined by comparing the density in
 256 the simulation with the estimated density. High accuracy is indicated by the mean
 257 difference between the estimated and actual values not being significantly differ-
 258 ent from zero (Wilcoxon signed-rank test). gREM precision was determined by
 259 the standard deviation of estimated densities. We used this method to compare
 260 the accuracy and precision of all the gREM submodels. As these submodels are
 261 derived for different combinations of α and θ , the accuracy and precision of the
 262 submodels was used to determine the impact of different values of α and θ .

263 The influence of the number of captures and animal movement models on ac-
 264 curacy and precision was investigated using four different gREM submodels rep-
 265 resentative of the range α and θ values (submodels NW1, SW1, NE1, and SE3,
 266 Figure 2). Using these four submodels, we calculated how long the simulation
 267 needed to run to generate a range of different capture numbers (from 10 to 100 cap-
 268 tures in 10 unit intervals), and estimated animal density. These estimated densities
 269 were compared to the real density to assess the impact on the accuracy and preci-
 270 sion of the gREM. We calculated the coefficient of variation in order to compare
 271 the precision between capture numbers. The gREM also assumes that individuals
 272 move continuously with straight-line movement (simple movement model) and
 273 we therefore assessed the impact of breaking the gREM assumptions. We used
 274 the four submodels to compare the accuracy and precision of a simple movement
 275 model, stop-start movement models (using different amounts of time spent sta-
 276 tionary), and random walk movement models.

RESULTS

Analytical model. The equation for \bar{p} has been newly derived for each submodel in the gREM, except for the gas model and REM which have been calculated previously. However, many models, although derived separately, have the same expression for \bar{p} . Figure 4 shows the expression for \bar{p} in each case. The general equation for density, using the correct expression for \bar{p} is then substituted into eqn 3. Although more thorough checks are performed in Appendix S3, it can be seen that all adjacent expressions in Figure 4 are equal when expressions for the boundaries between them are substituted in.

Simulation model.

gREM submodels. All gREM submodels showed a high accuracy, i.e., the mean difference between the estimated and actual values was not significantly different from zero across all models, at $p < 0.05$, corrected for multiple tests (all gREM submodels Wilcoxon signed-rank test) (Figure 5). However, the precision of the submodels do vary, where the gas model is the most precise and the SW7 sub model the least precise, having the smallest and the largest interquartile range, respectively (Figure 5). The standard deviation of the error between the estimated and true densities is strongly related to both the sensor and signal widths (Appendix S5), such that larger widths have lower standard deviations (greater precision).

Number of captures. Within the four gREM submodels tested (NW1, SW1, SE3, NE1), the accuracy was not affected by the number of captures. The mean difference between the estimated and actual values was not significantly different from zero across all capture rates, at $p < 0.05$, corrected for multiple tests (Wilcoxon signed-rank test) (Figure 6). However, the precision was dependent on the number of captures across all four of the gREM submodels, where precision increases as number of captures increases (Figure 6). For all gREM submodels, the coefficient of variation falls to 10% at 100 captures.

304 *Movement models.* Within the four gREM submodels tested (NW1, SW1, SE3, NE1),
 305 neither the accuracy or precision was affected by the amount of time spent station-
 306 ary. The mean difference between the estimated and actual values was not signifi-
 307 cantly different from zero for each category of stationary time (0, 0.25, 0.5 and 0.75),
 308 at $p < 0.05$, corrected for multiple tests (all gREM sub models Wilcoxon signed-
 309 rank test) (Figure 7a). Altering the maximum change in direction in each step (0,
 310 $\pi/3$, $2\pi/3$, and π) did not affect the accuracy or precision of the four gREM sub-
 311 models tested, at $p < 0.05$, corrected for multiple testing (Wilcoxon signed-rank
 312 test) (Figure 7b).

313 DISCUSSION

314 We have developed the gREM such that it can be used to estimate density from
 315 acoustic sensors and camera traps. This has entailed a generalisation of the gas
 316 model and the REM in Rowcliffe *et al.* (2008) to be applicable to any combination
 317 of sensor width and signal directionality. We have used simulations to show, as a
 318 proof of principle, that these models are accurate and precise. The precision of the
 319 gREM was found to be dependent on the width of the sensor and the signal, and
 320 the number of captures.

321 **Analytical model.** The gREM was derived for different combinations of α and θ
 322 resulting in 25 different submodels, the expression for \bar{p} are equal for many of
 323 these submodels resulting in eight different equations including the previously
 324 derived gas model and REM. These submodels were tested for consistency with
 325 adjacent expressions being equal at their boundaries. These new submodels will
 326 allow researchers to evaluate the absolute density of animals that have previously
 327 been difficult to study, such as echolocating bats (Clement & Castleberry, 2013),
 328 with non-invasive methods such as remote sensors. The gREM also allows the
 329 data from acoustic detectors to be used where an animal has a directional calls,
 330 this could be used for a range of animals including songbirds (Blumstein *et al.*,
 331 2011), dolphins (Lammers & Au, 2003), as well as echolocating bats (Walters *et al.*,
 332 2013).

333 There are a number of possible extensions to the gREM which could be devel-
 334 oped in the future. The original gas model was formulated for the case where both

subjects, either animal and detector, or animal and animal, are moving (Hutchinson & Waser, 2007). Indeed any of the models with animals that are equally detectable in all directions ($\alpha = 2\pi$) can be trivially expanded for moving by substituting the sum of the average animal velocity and the sensor velocity for v as used here. However, when the animal has a directional call, as seen in both terrestrial and aquatic environments (Lammers & Au, 2003; Blumstein *et al.*, 2011), the extension becomes less simple. The approach would be to calculate again the mean profile width. However, for each angle of approach, one would have to average the profile width for an animal facing in any direction (i.e., not necessarily moving towards the sensor) weighted by the relative velocity of that direction. There are a number of situations where a moving detector and animal could occur, e.g. an acoustic detector towed from a boat when studying porpoises (Kimura *et al.*, 2014) or surveying echolocating bats from a moving car (Ahlen & Baagøe, 1999; Jones *et al.*, 2013).

Interesting but unstudied problems impacting the gREM are firstly, edge effects caused by sensor trigger delays (the delay between sensing an animal and attempting to record the encounter) (Rovero *et al.*, 2013), and secondly, sensors which repeatedly turn on and off during sampling (Jones *et al.*, 2013). The second problem is particularly relevant to acoustic detectors which record ultrasound by time expansion. Here ultrasound is recorded for a set time period and then slowed down and played back, rendering the sensor 'deaf' periodically during sampling. Both of these problems may cause biases in the gREM, as animals can move through the detection zone without being detected. As the gREM assumes constant surveillance, the error created by switching the sensor on and off quickly will become more important if the sensor is only on for short periods of time. For example, if it takes longer for the recording device to be switched on than the length of some animal calls, then there could be a systematic underestimation of density. We recommend that the gREM is applied to constantly sampled data, and the impacts of breaking these assumptions on the gREM should be further explored.

Accuracy, Precision and Recommendations for Best Practice. Based on our simulations, we believe that the gREM has the potential to produce accurate estimates

for many different species, using either camera traps or acoustic detectors. However, the precision of the gREM differed between submodels. For example, when the sensor and signal width were small, the precision of the model was reduced. Therefore when choosing a sensor for use in a gREM study, the sensor detection width should be maximised. If the study species has a narrow signal directionality, other aspects of the study protocol, such as length of the survey, should be used to compensate.

The precision of the gREM is greatly affected by the number of captures. The coefficient of variation falls dramatically between 10 and 60 captures and then after this continues to slowly reduce. At 100 captures the submodels reach 10% coefficient of variation, considered to a very good level of precision (Thomas & Marques, 2012). Many current studies do not reach this level of precision, with most studies reporting coefficient of variations greater than the 10% level (O'Brien *et al.*, 2003; Proctor *et al.*, 2010; Foster & Harmsen, 2012). The length of surveys in the field will need to be adjusted so that enough data can be collected to reach this precision level. Populations of fast moving animals or populations with high densities will require less survey effort than those species that are slow moving or have populations with low densities.

The gREM was both accurate and precise for all the movement models we tested (stop-start movement and correlated random walks). However, these movement models are still simple representations of true animal movement which are dependent on multiple factors such as behavioural state and existence of home ranges (Smouse *et al.*, 2010). The accuracy of the gREM may be affected by the interaction between the movement model and the size of the detection radius. We have studied a relatively long step length compared to the size of the detection radius, and therefore the chance of catching the same animal multiple times within a short space of time was reduced and there is little effect on the precision of the model (Figure 7b). However, if the ratio of step length to detection radius was smaller, then this may decrease the precision of the model (but should not decrease its accuracy).

Limitations. Although we have used simulations to validate the gREM submodels, much more robust testing is needed. Although difficult, proper field test validation would be required before the models could be fully trusted. The REM (Rowcliffe *et al.*, 2008) has already been field tested, and both Rowcliffe *et al.* (2008) and Zero *et al.* (2013) both found that the REM was an effective manner of estimating animal densities (Rowcliffe *et al.*, 2008; Zero *et al.*, 2013). In some taxa gold standard methods of estimating animal density exist, such as capture mark recapture (Sollmann *et al.*, 2013). Where these gold standard exist or true numbers are known, a simultaneous gREM study could be completed to test the accuracy under field conditions, similar to the tests in Rowcliffe *et al.* (2008). An easier way to continue to evaluate the models is to run more extensive simulations which break the assumptions of the analytical models. The main element that cannot be analytically treated is the complex movement of real animals. Therefore testing these methods against true animal traces, or more complex movement models would be required.

Within the simulation we have assumed an equal density across the entire world, however in a field environment the situation would be much more complex, with additional variation coming from local changes in density between sensor sites. We allowed the sensor to be stationary and continuously detecting, negating the triggering, and non-continuous recording issues that could exist with some sensors. In the simulation, the distance travelled of animal was assumed to be 40 km day^{-1} , the largest day range of terrestrial animals (Carbone *et al.*, 2005). Other speed values should not alter the accuracy of the gREM, however, precision would be affected, all else being equal, since slower speeds produce fewer records. We also assume perfect knowledge of the average speed of an animal and size of the detection zone. All of which may lead to possible bias or a decrease in precision.

Implications for ecology and conservation. The gREM can estimate densities of a number of taxa where no, or few, accurate methods currently exist to measure absolute animal density and trends in absolute abundances (Thomas & Marques,

2012). Many of these species are critically endangered and monitoring their populations is of conservation interest. For example, current methods of density estimation for the threatened Franciscana dolphin (*Pontoporia blainvillei*) may result in underestimation of their numbers (Crespo *et al.*, 2010). Our method may also be important for understanding zoonotic diseases, for example estimating population sizes of echolocating bats, which are important reservoir of infectious disease that affect humans, livestock and wildlife (Calisher *et al.*, 2006). In addition, the gREM will make it possible to measure the density of animals which may be useful in quantifying ecosystem services, such as studying the levels of songbirds which are known to have a positive influence on pest control in coffee production (Jirinec *et al.*, 2011). The gREM is suitable for any species that would be consistently recorded within range of a detector, such as echolocating bats (Kunz *et al.*, 2009), songbirds (Buckland & Handel, 2006), whales (Marques *et al.*, 2009) or forest primates (Hassel-Finnegan *et al.*, 2008). With increasing technological capabilities, this list of species is likely to increase dramatically. Finally, the passive sensor methods that the gREM use are noninvasive and do not require individual marking (Jewell, 2013) or naturally identifying marks (as required for mark-recapture models). This makes them suitable for large, continuous monitoring projects with limited human resources (Kelly *et al.*, 2012). It also makes them suitable for species that are under pressure, species that cannot naturally be individually recognised or species that are difficult or dangerous to catch (Thomas & Marques, 2012).

ACKNOWLEDGMENTS

We thank Hilde Wilkinson-Herbot, Chris Carbone, Francois Balloux, Andrew Cunningham, and Steve Hailes for comments on previous versions of the manuscript. This study was funded through CoMPLEX PhD studentships at University College London supported by BBSRC and EPSRC (EAM and TCDL); The Darwin Initiative (Awards 15003, 161333, EIDPR075 to KEJ), and The Leverhulme Trust (Philip Leverhulme Prize for KEJ).

REFERENCES

- Acevedo, M.A. & Villanueva-Rivera, L.J. (2006) Using automated digital recording systems as effective tools for the monitoring of birds and amphibians. *Wildlife Society Bulletin*, **34**, 211–214.
- Ahlen, I. & Baagøe, H.J. (1999) Use of ultrasound detectors for bat studies in europe: experiences from field identification, surveys, and monitoring. *Acta Chiropterologica*, **1**, 137–150.
- Anderson, D.R. (2001) The need to get the basics right in wildlife field studies. *Wildlife Society Bulletin*, **29**, 1294–1297.
- Barlow, J. & Taylor, B. (2005) Estimates of sperm whale abundance in the north-eastern temperate pacific from a combined acoustic and visual survey. *Marine Mammal Science*, **21**, 429–445.
- Blumstein, D.T., Mennill, D.J., Clemins, P., Girod, L., Yao, K., Patricelli, G., Deppe, J.L., Krakauer, A.H., Clark, C., Cortopassi, K.A. *et al.* (2011) Acoustic monitoring in terrestrial environments using microphone arrays: applications, technological considerations and prospectus. *Journal of Applied Ecology*, **48**, 758–767.
- Borchers, D., Distiller, G., Foster, R., Harmsen, B. & Milazzo, L. (2014) Continuous-time spatially explicit capture–recapture models, with an application to a jaguar camera-trap survey. *Methods in Ecology and Evolution*, **5**, 656–665.
- Brusa, A. & Bunker, D.E. (2014) Increasing the precision of canopy closure estimates from hemispherical photography: Blue channel analysis and under-exposure. *Agricultural and Forest Meteorology*, **195**, 102–107.
- Buckland, S.T. & Handel, C. (2006) Point-transect surveys for songbirds: robust methodologies. *The Auk*, **123**, 345–357.
- Buckland, S.T., Marsden, S.J. & Green, R.E. (2008) Estimating bird abundance: making methods work. *Bird Conservation International*, **18**, S91–S108.
- Calisher, C., Childs, J., Field, H., Holmes, K. & Schountz, T. (2006) Bats: important reservoir hosts of emerging viruses. *Clinical Microbiology Reviews*, **19**, 531–545.
- Carbone, C., Cowlshaw, G., Isaac, N.J. & Rowcliffe, J.M. (2005) How far do animals go? Determinants of day range in mammals. *The American Naturalist*, **165**, 290–297.

- 484 Clark, C.W. (1995) Application of US Navy underwater hydrophone arrays for
485 scientific research on whales. *Reports of the International Whaling Commission*, **45**,
486 210–212.
- 487 Clement, M.J. & Castleberry, S.B. (2013) Estimating density of a forest-dwelling
488 bat: a predictive model for rafinesque’s big-eared bat. *Population Ecology*, **55**,
489 205–215.
- 490 Crespo, E.A., Pedraza, S.N., Grandi, M.F., Dans, S.L. & Garaffo, G.V. (2010) Abun-
491 dance and distribution of endangered franciscana dolphins in argentine waters
492 and conservation implications. *Marine Mammal Science*, **26**, 17–35.
- 493 Cutler, T.L. & Swann, D.E. (1999) Using remote photography in wildlife ecology:
494 a review. *Wildlife Society Bulletin*, **27**, 571–581.
- 495 Damuth, J. (1981) Population density and body size in mammals. *Nature*, **290**,
496 699–700.
- 497 Depraetere, M., Pavoine, S., Jiguet, F., Gasc, A., Duvail, S. & Sueur, J. (2012) Mon-
498 itoring animal diversity using acoustic indices: implementation in a temperate
499 woodland. *Ecological Indicators*, **13**, 46–54.
- 500 Elphick, C.S. (2008) How you count counts: the importance of methods research
501 in applied ecology. *Journal of Applied Ecology*, **45**, 1313–1320.
- 502 Everatt, K.T., Andresen, L. & Somers, M.J. (2014) Trophic scaling and occupancy
503 analysis reveals a lion population limited by top-down anthropogenic pressure
504 in the limpopo national park, mozambique. *PloS one*, **9**, e99389.
- 505 Foster, R.J. & Harmsen, B.J. (2012) A critique of density estimation from camera-
506 trap data. *The Journal of Wildlife Management*, **76**, 224–236.
- 507 Harris, D., Matias, L., Thomas, L., Harwood, J. & Geissler, W.H. (2013) Applying
508 distance sampling to fin whale calls recorded by single seismic instruments in
509 the northeast atlantic. *The Journal of the Acoustical Society of America*, **134**, 3522–
510 3535.
- 511 Hassel-Finnegan, H.M., Borries, C., Larney, E., Umponjan, M. & Koenig, A. (2008)
512 How reliable are density estimates for diurnal primates? *International Journal of*
513 *Primatology*, **29**, 1175–1187.

- 514 Hayes, J.P. (2000) Assumptions and practical considerations in the design and in-
515 terpretation of echolocation-monitoring studies. *Acta Chiropterologica*, **2**, 225–
516 236.
- 517 Hutchinson, J.M.C. & Waser, P.M. (2007) Use, misuse and extensions of “ideal gas”
518 models of animal encounter. *Biological Reviews of the Cambridge Philosophical So-*
519 *ciet*y, **82**, 335–359.
- 520 Jewell, Z. (2013) Effect of monitoring technique on quality of conservation science.
521 *Conservation Biology*, **27**, 501–508.
- 522 Jirinec, V., Campos, B.R. & Johnson, M.D. (2011) Roosting behaviour of a migratory
523 songbird on jamaican coffee farms: landscape composition may affect delivery
524 of an ecosystem service. *Bird Conservation International*, **21**, 353–361.
- 525 Jones, K.E., Bielby, J., Cardillo, M., Fritz, S.A., O’Dell, J., Orme, C.D.L., Safi, K.,
526 Sechrest, W., Boakes, E.H., Carbone, C., Connolly, C., Cutts, M.J., Foster, J.K.,
527 Grenyer, R., Habib, M., Plaster, C.A., Price, S.A., Rigby, E.A., Rist, J., Teacher,
528 A., Bininda-Emonds, O.R.P., Gittleman, J.L., Mace, G.M., Purvis, A. & Michener,
529 W.K. (2009) Pantheria: a species-level database of life history, ecology, and ge-
530 ography of extant and recently extinct mammals. *Ecology*, **90**, 2648.
- 531 Jones, K.E., Russ, J.A., Bashta, A.T., Bilhari, Z., Catto, C., Csősz, I., Gorbachev,
532 A., Győrfi, P., Hughes, A., Ivashkiv, I., Koryagina, N., Kurali, A., Langton, S.,
533 Collen, A., Margiean, G., Pandourski, I., Parsons, S., Prokofev, I., Szodoray-
534 Paradi, A., Szodoray-Paradi, F., Tilova, E., Walters, C.L., Weatherill, A. &
535 Zavarzin, O. (2013) Indicator bats program: A system for the global acoustic
536 monitoring of bats. B. Collen, N. Pettorelli, J.E.M. Baillie & S.M. Durant, eds.,
537 *Biodiversity Monitoring and Conservation*, pp. 211–247. Wiley-Blackwell.
- 538 Karanth, K. (1995) Estimating tiger (*Panthera tigris*) populations from camera-trap
539 data using capture–recapture models. *Biological Conservation*, **71**, 333–338.
- 540 Kelly, M.J., Betsch, J., Wultsch, C., Mesa, B. & Mills, L.S. (2012) Noninvasive sam-
541 pling for carnivores. *Carnivore ecology and conservation: a handbook of techniques*
542 (*L Boitani and RA Powell, eds*) Oxford University Press, New York, pp. 47–69.
- 543 Kessel, S., Cooke, S., Heupel, M., Hussey, N., Simpfendorfer, C., Vagle, S. & Fisk, A.
544 (2014) A review of detection range testing in aquatic passive acoustic telemetry
545 studies. *Reviews in Fish Biology and Fisheries*, **24**, 199–218.

- 546 Kimura, S., Akamatsu, T., Dong, L., Wang, K., Wang, D., Shibata, Y. & Arai, N.
547 (2014) Acoustic capture-recapture method for towed acoustic surveys of echolo-
548 cating porpoises. *The Journal of the Acoustical Society of America*, **135**, 3364–3370.
- 549 Kunz, T.H., Betke, M., Hristov, N.I. & Vonhof, M. (2009) Methods for assessing
550 colony size, population size, and relative abundance of bats. *Ecological and be-
551 havioral methods for the study of bats (TH Kunz and S Parsons, eds) 2nd ed Johns
552 Hopkins University Press, Baltimore, Maryland*, pp. 133–157.
- 553 Lammers, M.O. & Au, W.W. (2003) Directionality in the whistles of hawaiian spin-
554 ner dolphins (*stenella longirostris*): A signal feature to cue direction of move-
555 ment? *Marine Mammal Science*, **19**, 249–264.
- 556 Lewis, T., Gillespie, D., Lacey, C., Matthews, J., Danbolt, M., Leaper, R.,
557 McLanaghan, R. & Moscrop, A. (2007) Sperm whale abundance estimates from
558 acoustic surveys of the ionian sea and straits of sicily in 2003. *Journal of the Ma-
559 rine Biological Association of the United Kingdom*, **87**, 353–357.
- 560 Manzo, E., Bartolommei, P., Rowcliffe, J.M. & Cozzolino, R. (2012) Estimation of
561 population density of european pine marten in central italy using camera trap-
562 ping. *Acta Theriologica*, **57**, 165–172.
- 563 Marcoux, M., Auger-Méthé, M., Chmelnitsky, E.G., Ferguson, S.H. & Humphries,
564 M.M. (2011) Local passive acoustic monitoring of narwhal presence in the cana-
565 dian arctic: a pilot project. *Arctic*, **64**, 307–316.
- 566 Marques, T.A., Munger, L., Thomas, L., Wiggins, S. & Hildebrand, J.A. (2011) Es-
567 timating North Pacific right whale (*Eubalaena japonica*) density using passive
568 acoustic cue counting. *Endangered Species Research*, **13**, 163–172.
- 569 Marques, T.A., Thomas, L., Ward, J., DiMarzio, N. & Tyack, P.L. (2009) Estimating
570 cetacean population density using fixed passive acoustic sensors: An example
571 with Blainville’s beaked whales. *The Journal of the Acoustical Society of America*,
572 **125**, 1982–1994.
- 573 O’Brien, T.G., Kinnaird, M.F. & Wibisono, H.T. (2003) Crouching tigers, hidden
574 prey: Sumatran tiger and prey populations in a tropical forest landscape. *Animal
575 Conservation*, **6**, 131–139.
- 576 Proctor, M., McLellan, B., Boulanger, J., Apps, C., Stenhouse, G., Paetkau, D. &
577 Mowat, G. (2010) Ecological investigations of grizzly bears in canada using dna

- 578 from hair, 1995-2005: a review of methods and progress. *Ursus*, **21**, 169–188.
- 579 Purvis, A., Gittleman, J.L., Cowlishaw, G. & Mace, G.M. (2000) Predicting extinc-
580 tion risk in declining species. *Proceedings of the Royal Society of London Series B:*
581 *Biological Sciences*, **267**, 1947–1952.
- 582 Richter-Dyn, N. & Goel, N.S. (1972) On the extinction of a colonizing species. *The-*
583 *oretical Population Biology*, **3**, 406–433.
- 584 Rogers, T.L., Ciaglia, M.B., Klinck, H. & Southwell, C. (2013) Density can be mis-
585 leading for low-density species: benefits of passive acoustic monitoring. *Public*
586 *Library of Science One*, **8**, e52542.
- 587 Rovero, F., Zimmermann, F., Berzi, D. & Meek, P. (2013) “Which camera trap type
588 and how many do I need?” a review of camera features and study designs for a
589 range of wildlife research applications. *Hystrix*, **24**, 148–156.
- 590 Rowcliffe, J.M. & Carbone, C. (2008) Surveys using camera traps: are we looking
591 to a brighter future? *Animal Conservation*, **11**, 185–186.
- 592 Rowcliffe, J., Field, J., Turvey, S. & Carbone, C. (2008) Estimating animal density
593 using camera traps without the need for individual recognition. *Journal of Ap-*
594 *plied Ecology*, **45**, 1228–1236.
- 595 Schmidt, B.R. (2003) Count data, detection probabilities, and the demography, dy-
596 namics, distribution, and decline of amphibians. *Comptes Rendus Biologies*, **326**,
597 119–124.
- 598 Smouse, P.E., Focardi, S., Moorcroft, P.R., Kie, J.G., Forester, J.D. & Morales, J.M.
599 (2010) Stochastic modelling of animal movement. *Philosophical Transactions of the*
600 *Royal Society B: Biological Sciences*, **365**, 2201–2211.
- 601 Sollmann, R., Gardner, B., Chandler, R.B., Shindle, D.B., Onorato, D.P., Royle, J.A.
602 & O’Connell, A.F. (2013) Using multiple data sources provides density estimates
603 for endangered florida panther. *Journal of Applied Ecology*, **50**, 961–968.
- 604 SymPy Development Team (2014) *SymPy: Python library for symbolic mathematics*.
605 Team, R.C. (2014) *R: A Language and Environment for Statistical Computing*. R Foun-
606 dation for Statistical Computing, Vienna, Austria.
- 607 Thomas, L. & Marques, T.A. (2012) Passive acoustic monitoring for estimating an-
608 imal density. *Acoustics Today*, **8**, 35–44.

- 609 Trolle, M., Noss, A.J., Lima, E.D.S. & Dalponte, J.C. (2007) Camera-trap studies of
610 maned wolf density in the Cerrado and the Pantanal of Brazil. *Biodiversity and*
611 *Conservation*, **16**, 1197–1204.
- 612 Walters, C.L., Collen, A., Lucas, T., Mroz, K., Sayer, C.A. & Jones, K.E. (2013) Chal-
613 lenges of using bioacoustics to globally monitor bats. R.A. Adams & S.C. Ped-
614 ersen, eds., *Bat Evolution, Ecology, and Conservation*, pp. 479–499. Springer.
- 615 Walters, C.L., Freeman, R., Collen, A., Dietz, C., Brock Fenton, M., Jones, G., Obrist,
616 M.K., Puechmaille, S.J., Sattler, T., Siemers, B.M. *et al.* (2012) A continental-scale
617 tool for acoustic identification of european bats. *Journal of Applied Ecology*, **49**,
618 1064–1074.
- 619 Wright, S.J. & Hubbell, S.P. (1983) Stochastic extinction and reserve size: a focal
620 species approach. *Oikos*, pp. 466–476.
- 621 Yapp, W. (1956) The theory of line transects. *Bird Study*, **3**, 93–104.
- 622 Zero, V.H., Sundaresan, S.R., O'Brien, T.G. & Kinnaird, M.F. (2013) Monitoring
623 an endangered savannah ungulate, Grevy's zebra (*Equus grevyi*): choosing a
624 method for estimating population densities. *Oryx*, **47**, 410–419.

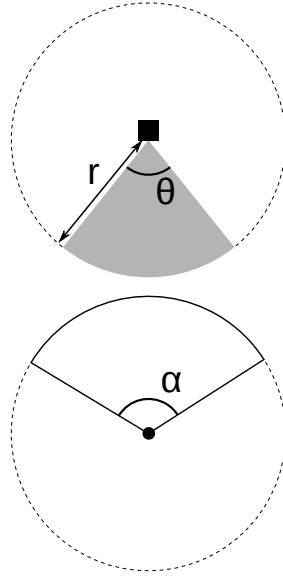


Figure 1. Representation of sensor detection width and animal signal width. The filled square and circle represent a sensor and an animal, respectively; θ , sensor detection width (radians); r , sensor detection distance; dark grey shaded area, sensor detection zone; α , animal signal width (radians). Dashed lines around the filled square and circle represents the maximum extent of θ and α , respectively.

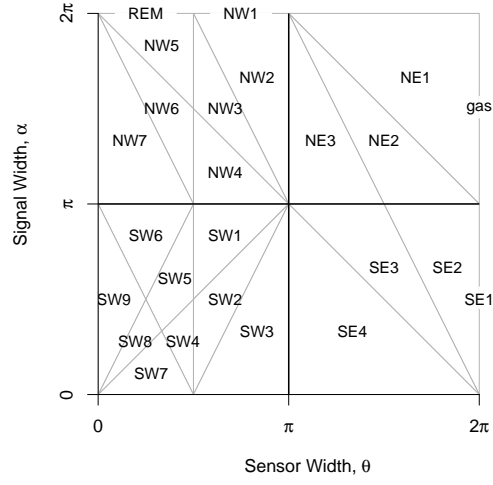


Figure 2. Locations where derivation of the average profile \bar{p} is the same for different combinations of sensor detection and animal signal widths. Symbols within each polygon refer to each gREM submodel named after their compass point, except for Gas and REM which highlight the position of these previously derived models within the gREM. Symbols on the edge of the plot are for submodels where $\alpha, \theta = 2\pi$

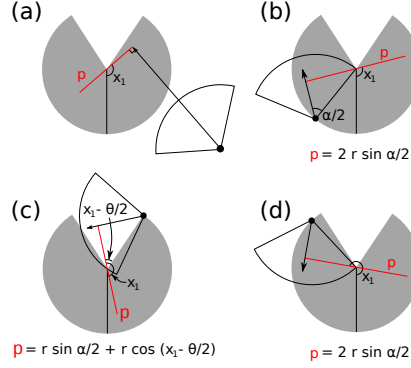


Figure 3. An overview of the derivation of the average profile \bar{p} for the gREM submodel SE2, where (a) shows the location of the profile p (the line an animal must pass through in order to be captured) in red and the focal angle, x_1 , for an animal (filled circle), its signal (unfilled sector), and direction of movement (shown as an arrow). The detection zone of the sensor is shown as a filled grey sector with a detection distance of r . The vertical black line within the circle shows the direction the sensor is facing. The derivation of p changes as the animal approaches the sensor from different directions (shown in b-d), where (b) is the derivation of p when x_1 is in the interval $[\frac{\pi}{2}, \frac{\pi}{2} + \frac{\theta}{2} - \frac{\alpha}{2}]$, (c) p when x_1 is in the interval $[\frac{\pi}{2} + \frac{\theta}{2} - \frac{\alpha}{2}, \frac{5\pi}{2} - \frac{\theta}{2} - \frac{\alpha}{2}]$ and (d) p when x_1 is in the interval $[\frac{5\pi}{2} - \frac{\theta}{2} - \frac{\alpha}{2}, \frac{3\pi}{2}]$, where θ , sensor detection width; α , animal signal width. The resultant equation for p is shown beneath b-d. The average profile \bar{p} is the size of the profile averaged across all approach angles.

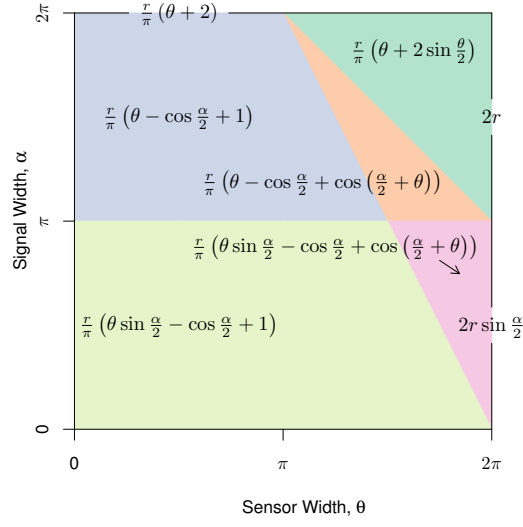


Figure 4. Expressions for the average profile width, \bar{p} , given a range of sensor and signal widths. Despite independent derivation within each block, many models result in the same expression. These are collected together and presented as one block of colour. Expressions on the edge of the plot are for submodels with $\alpha, \theta = 2\pi$.

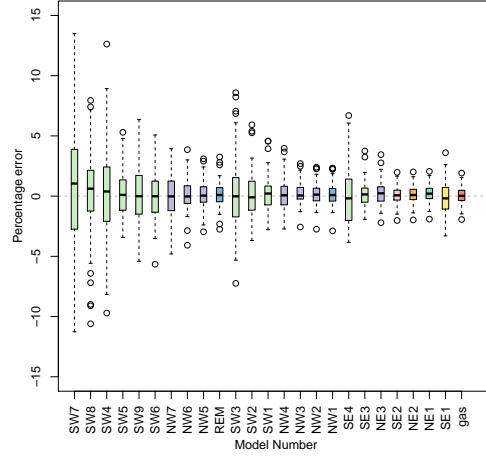


Figure 5. Simulation model results of the accuracy and precision for gREM submodels. The percentage error between estimated and true density for each gREM sub model is shown within each box plot, where the black line represents the median percentage error across all simulations, boxes represent the middle 50% of the data, whiskers represent variability outside the upper and lower quartiles with outliers plotted as individual points. Box colours correspond to the expressions for average profile width \bar{p} given in Figure 4.

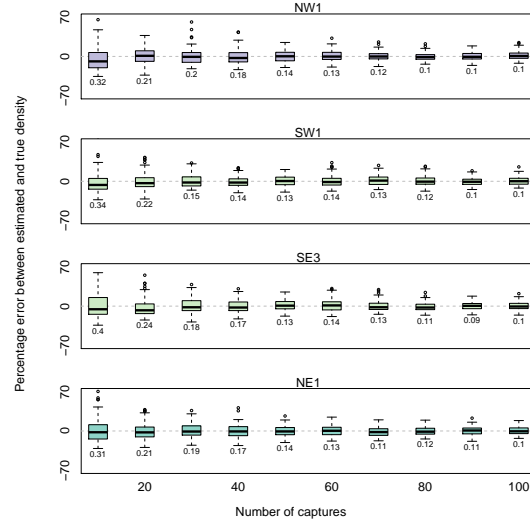


Figure 6. Simulation model results of the accuracy and precision of four gREM submodels (NW1, SW1, SE3 and NE1) given different numbers of captures. The percentage error between estimated and true density within each gREM sub model for capture rate is shown within each box plot, where the black line represents the median percentage error across all simulations, boxes represent the middle 50% of the data, whiskers represent variability outside the upper and lower quartiles with outliers plotted as individual points. Sensor and signal widths vary between submodels. The numbers beneath each plot represent the coefficient of variation. The colour of each box plot corresponds to the expressions for average profile width \bar{p} given in Figure 4.

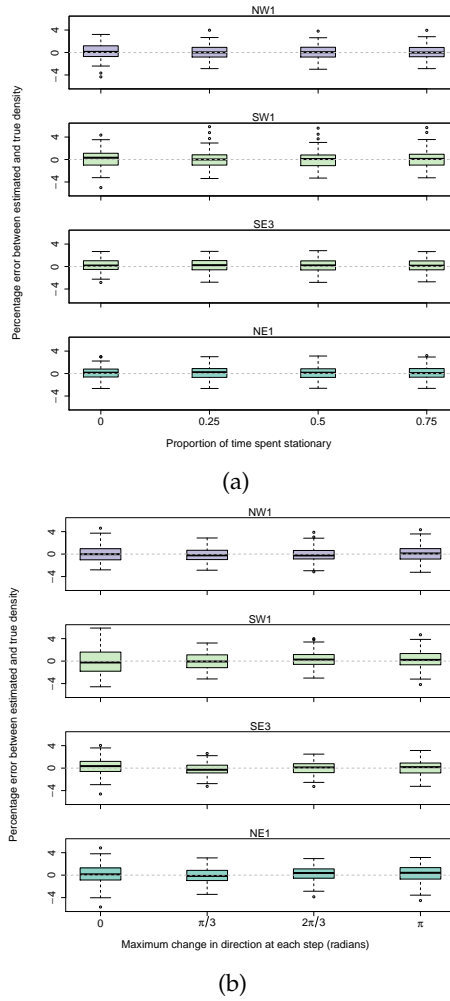


Figure 7. Simulation model results of the accuracy and precision of four gREM submodels (NW1, SW1, SE3 and NE1) given different movement models where (a) amount of time spent stationary (stop-start movement) and (b) maximum change in direction at each step (correlated random walk model). The percentage error between estimated and true density within each gREM sub model for the different movement models is shown within each box plot, where the black line represents the median percentage error across all simulations, boxes represent the middle 50% of the data, whiskers represent variability outside the upper and lower quartiles with outliers plotted as individual points. The simple model is represented where time and maximum change in direction equals 0. The colour of each box plot corresponds to the expressions for average profile width \bar{p} given in Figure 4.